A two-phase geothermal wellbore simulator to model THC behavior using Elmer-PHREEQC

Yodha Y. Nusiaputra[1], Alain Dimier[2], Thomas Kohl[1]

[1] Karlsruhe Institute of Technology, Institute of Applied Geosciences, 76131 Karlsruhe, Germany

[2] European Institute for Energy Research, 76131 Karlsruhe, Germany

yodha.nusiaputra@kit.edu

Keywords: Multicomponent flow; Transient; Deep geothermal wellbores; Thermohydro-chemical; operator splitting algorithm

ABSTRACT

The thermohydraulic-chemical (THC) behavior of a deep geothermal wellbore can be seriously affected by two-phase flow effect. In geothermal wellbore with high non-condensable gas content applications, this situation may lead to inaccurate pressure, temperature, and mineral saturation index calculation. However, due to the complexity of describing this effect, it is normally not considered in the modeling process. A method for calculating the transport and (de)pressurization with a thermal load of a two-phase multi-component geothermal fluid is presented. The thermodynamical and transport properties for an H2O - salt (NaCl, CaCl2, KCl, MgCl2, NaHCO3) - gas (CO2, N2, CH4, H2S) mixture are calculated using the fugacity-activity, three-zone Equation of State. The fluid flow is described by a heterogeneous drift-flux model, which is solved using the Elmer FEM. An operator splitting algorithm is applied to couple PHREEQC for calculating chemical reaction. Numerical results are shown, illustrating the effect of mixture composition and the feasibility of the approach.

1. INTRODUCTION

Mineral deposition in the wellbore not only jams the equipment and pipeline, but also gets heavy corrosion of down-hole's pipe string and rig on ground. The accurate prediction of mineral deposition in the well bore is very important. Because minerals solubility is a function of temperature and pressure in the high sulfur gas well bore, this paper addressed solubility mode of minerals to build up deposition's prediction model after we had simulated on pressure and temperature under these different flows. In order to resolve above issue and achieve performance prediction of sulfur deposition, basing on Sulfur solubility being a function of temperature and pressure in the high sulfur gas well bore, grain mechanics analysis under difference flow pattern was introduced to build up mineral deposition's prediction model in this article, assuming transient stable flow in the wellbore and non-stable heat transfer process. Sensitivity analysis was carried out to examine the impact of each wellbore parameters.

2. THE TWO-PHASE ONE-DIMENSIONAL WELLBORE PROBLEM

Generally, two basic geometries can be considered for wellbores, including one or two strings with the downward or upward flow and multiple tubing layers. In this work, one string with down/upward flow is studied.

The scope of this work is limited to practical situations that fit the following simplifying assumptions:

1. A quasi-steady-state analysis for mass balance is performed.
2. All chemical reactions and thermodynamic states are in equilibrium.
3. Axial conduction, radiative heat transfer, and ambient temperature effects are negligibly small.

The general modeling for the evolution of the streams is based on one-dimensional mass, momentum and energy balances for each string. Then, the problem is governed by Eqs. (1) – (4) for one string, which represents momentum and energy balances for fluid and rock. Heterogeneous model, VDI Heat Atlas, 2010 with void fraction correlation from Hasan-Kabir, 2002.

$$A\frac{\partial \rho_H}{\partial t} + sin\theta \frac{\partial \dot{m}}{\partial z} = 0 \qquad (1)$$

Time step in geothermal wellbore operation typically has a larger value (Δt > 1 min.). The simulation assumes the following thermal transport mechanisms: transient change of heat content, advection and heat transfer which are partially equilibrium. These may be written as follows

$$A\frac{\partial}{\partial t}(\varepsilon\rho^{NA}h^{NA}+(1-\varepsilon)\rho^{AQ}h^{AQ}) + sin\theta\frac{\partial}{\partial z}\left(\dot{m}\left(h+\frac{\dot{m}^2}{2A^2\rho_E^2}\right)\right) = A\frac{\partial p}{\partial t}-\dot{m}g\cdot sin\theta - \frac{\dot{m}}{\rho_H}\Delta p_f + P\dot{q}_w \quad (2)$$

, with the mixed enthalpy is defined as

$$h = xh^{NA}+(1-x)h^{AQ} \quad (3)$$

and in the formation matrix, diffusion with the transient term is written as

$$A_w\rho_r c_{p,r}\cdot\left(\frac{\partial T}{\partial t}+v_r\cdot\nabla T\right)-\nabla\cdot(\lambda\nabla T)=0 \quad (4)$$

Where T is temperature, t is time, c_p is specific heat capacity of fluid/rock media, λ is thermal conductivity of fluid/rock media, v is Darcy velocity, h is heat transfer coefficient, A is a cross-section of heat transfer, and V is volume.

Momentum balance is written as Navier-Stokes equation for 1D problem which could be closed with empirical equations for the shear stress, i.e. frictional pressure drop.

$$\frac{1}{A}\frac{\partial\dot{m}}{\partial t}+sin\theta\frac{\partial p}{\partial z} = -\rho_H g sin\theta-\Delta p_f - \frac{1}{A^2}\frac{\partial}{\partial z}\left(\frac{\dot{m}^2}{\rho_I}\right) \quad (5)$$

The time derivative of the momentum of the control volume $\partial\dot{m}/\partial t$ is assumed to be zero which is reasonable as long as fast dynamic processes (e.g., sound propagation) are not considered (see Casella and Leva, 2006).

The time derivative of the momentum of the control volume is assumed to be zero which is reasonable as long as fast dynamic processes (e.g., sound propagation) are not considered. To solve this system of equations, the coupling between enthalpy and mainly the density make the system non-linear and thus the iterative solution is required.

The gas-liquid mixture properties are modeled using mechanistic two-phase flow model from Hasan-Kabir, 2010, which also include slip between gas-fluid velocities. Bubbly, slug, churn and annular flow. The constitutive equations of hydraulic, thermal, and chemical to close all the equation systems above is explained below in detail..

2.1 Heat transfer models

Energy or thermal exchange is driven by temperature difference between fluid and rock/formation:

$$\dot{q}_w = U\cdot\left(T_f-T_w\right)\big|_{r=r_t} \quad (6)$$

Where UA is the linear heat transfer coefficient between rock at wellbore skin and geothermal brine stream. In a steady-state analysis, it can be computed on the base of thermal resistances (Incropera and DeWitt, 1996), which also can be used for transient analysis (Richter, 2008). Eq. (10) applies for the geometry shown in Fig. 1.

$$\frac{1}{U}=\frac{1}{h_t}+\frac{r_t ln\left(d_{o,t}/d_{i,t}\right)}{2\pi\lambda_t}+\frac{r_t}{r_a h_a} \quad (7)$$

with U is overall heat transfer coefficient, P is wet perimeter, h is convection HTC, k, is thermal conductivity, and n is a thermal layer, i.e. fluid stream, tubing, annulus, casing, cement.

Single phase, supercritical.

$$\frac{\alpha^{AQ}\cdot D_h}{k} = \begin{cases} 1.86\left(RePr\frac{D_h}{L}\right)^{0.33}, Re\le 2300 \\ 0.027Re^{0.8}Pr^{0.33}, Re>2300 \text{ or } p>22MPa \end{cases} \quad (8)$$

The non-boiling two-phase correlation was used as recommended by Ghajar, 2010 for oil-gas applications and regardless of flow-regime and Nusselt number. It can be written as

$$\alpha_{tp} = F_p\cdot\alpha^{AQ}\left[1+0.55\left(\frac{x}{1-x}\right)^{0.1}\left(\frac{1-F_p}{F_p}\right)^{0.4}\times\left(\frac{Pr^{NA}}{Pr^{AQ}}\right)^{0.25}\left(\frac{\mu^{NA}}{\mu^{AQ}}\right)^{0.25}(I^*)^{0.25}\right] \quad (9)$$

where α^{AQ} is computed using correlation from Sieder-Tate, 1936. Shah-Chen correlations for boiling two-phase heat transfer. The detailed description of the correlations are given in the Appendix.

$$\alpha_{tp} = \begin{cases} \alpha_{nb}S+\alpha^{AQ}F, \text{for } Fr\ge 0.04 \\ \alpha^{AQ}[c_1+c_2Bo^{0.5}exp(c_3)], \text{for } Fr<0.04 \end{cases} \quad (10)$$

2.2 Pressure drop models

Hydrostatic pressure holds the main role of the hydraulic system with density variation as the variable. This part is already included as a term in the momentum balance equation above related to wellbore deviation angle, θ.

Flow inside tubes is imposed by the pressure drop in the same direction of the mass flow rate due to shear stress with the tube surface. The shear stress is modeled on the base of a two-phase multiplier. In the following is the application of equations for the frictional pressure drop of two-phase tube flow. The frictional term is a part of momentum balance equation

$$\Delta p_f = f_H \frac{\dot{m}^2}{2A^2 \rho_H D_h} \tag{11}$$

where f is Darcy friction factor and ρ_m is mixture average density as function of fluid properties and flow conditions.

Investigations of the hydraulic behavior in pipes from the early century. Schlichting, 1979 describe the studies. In this study, Fang, 2011 is taken to take into account scaling and corrosion effect to the friction factor.

$$f_H = 1.16\left[ln\left(0.234Rr^{1.1007} - \frac{60.525}{Re_H^{1.1105}} + \frac{56.291}{Re_H^{1.0712}}\right)\right]^{-2} \tag{12}$$

with the Reynolds number is defined as

$$Re_H = \frac{\dot{m} D_h}{A \mu_H} \tag{13}$$

The correlations are valid for bubbly and slug flow. For annular flow, a film factor correction factor is required and can be written as [HasanKabir02]

$$\lambda_c = \lambda \cdot [1 + 75(1 - \varepsilon)] \tag{14}$$

where ε is the void fraction. Productivity index is modeled by the correlations.

2.3 Geochemical reaction models

For aqueous phase. The mass balance of N species per volume of medium may be defined as (Yeh-Tripathi, 1989)

$$\psi \frac{\partial T}{\partial t} + \frac{\partial \psi}{\partial t}(S + P) = L(C) + \psi r_{kin} \tag{15}$$

$$\psi \frac{\partial W}{\partial t} + \frac{\partial \psi}{\partial t} W = 0 \tag{16}$$

Which has two components: aqueous (mobile) and sorbent (immobile) component as written in Eq. and Eq. . θ is the moisture content, t is the time, L is advection-diffusion operator; C, S, P, and T are the total dissolved concentration, total sorbed concentration, total precipitated concentration, and total analytical concentration, respectively; W is the total analytical concentration of the sorbed component.

It is beyond the scope of this paper to describe all the equations that PHREEQC uses to represent chemical reactions. The complete formulation can be found in the PHREEQC manual (Parkhurst and Appelo, 1999). In general, a geochemical PHREEQC batch problem can be formulated as a differential algebraic equation (DAE) system of index 1 of the following form:

$$\frac{du_g}{dt} + \frac{du_m}{dt} + \frac{du_a}{dt} + \frac{du_d}{dt} = r_{kin} = 0 \tag{17}$$

$$f(u, c, T) = 0$$

The system consists of a set of ordinary differential equations (ODE) associated with kinetic reactions, and asset of algebraic equations which arise from the formulation of components u, the mass action law, the water activity model used to represent non-ideal solutions, etc. Furthermore, it includes the expressions (that are usually highly non-linear) that relate u, c, and T for non-isothermal problems. r_{kin} is assumed to be zero in this study to simplify the modeling. However, some minerals often do not react to equilibrium during the predefined time frame (Orywall, 2015). We recommend to model it when the situation demands.

To model geothermal brine at high temperature and pressure, "gebo" database (Bozau, 2013) is added and includes additional solution master species, which are Fe, Fe(+2), Fe(+3), S(−2), N, N(+5), N(+3), N(0), N(−3), C(−4), Si, Zn, Pb, and Al. According to this solution master species, associated solution species, solid phases, and gasses, as well as temperature dependences of the appropriate mass action law constants and Pitzer parameters for the calculation of activity coefficients in aqueous solutions of high ionic strength are implemented. In contrast to the conventional "pitzer.dat" database, the extended version allows calculating several additional hydrogeochemical equilibrium reactions that are required.

2.4 Thermodynamics

Liquid-like (aqueous), that may include dissolved hydrocarbons (here methane) and gases in addition to water and dissolved solids and gas-like (non-aqueous), basically a multi-component mixture that can be in gas, supercritical or condensed conditions phases partitioning. We use improved Duan-Sun model for gas solubilities. The EoS does not include solid/minerals as a separate phase.

3. NUMERICAL APPROACH

3.1 Technical description of Elmer - PHREEQC coupling

For a specified time step, Elmer calculates the progression of the system during this time step and

gives the result. PHREEQC calculates the chemical reaction at this step, based on the initial chemical state and on Elmer's result, and writes the result. Elmer now knows the new chemical state of each cell, and can re-calculate physical changes, such as the flow and dispersion during the time step. Again, PHREEQC will calculate the chemical equilibrium at this point, and this will continue until the end of the simulation. The smaller the time step, the greater the precision.

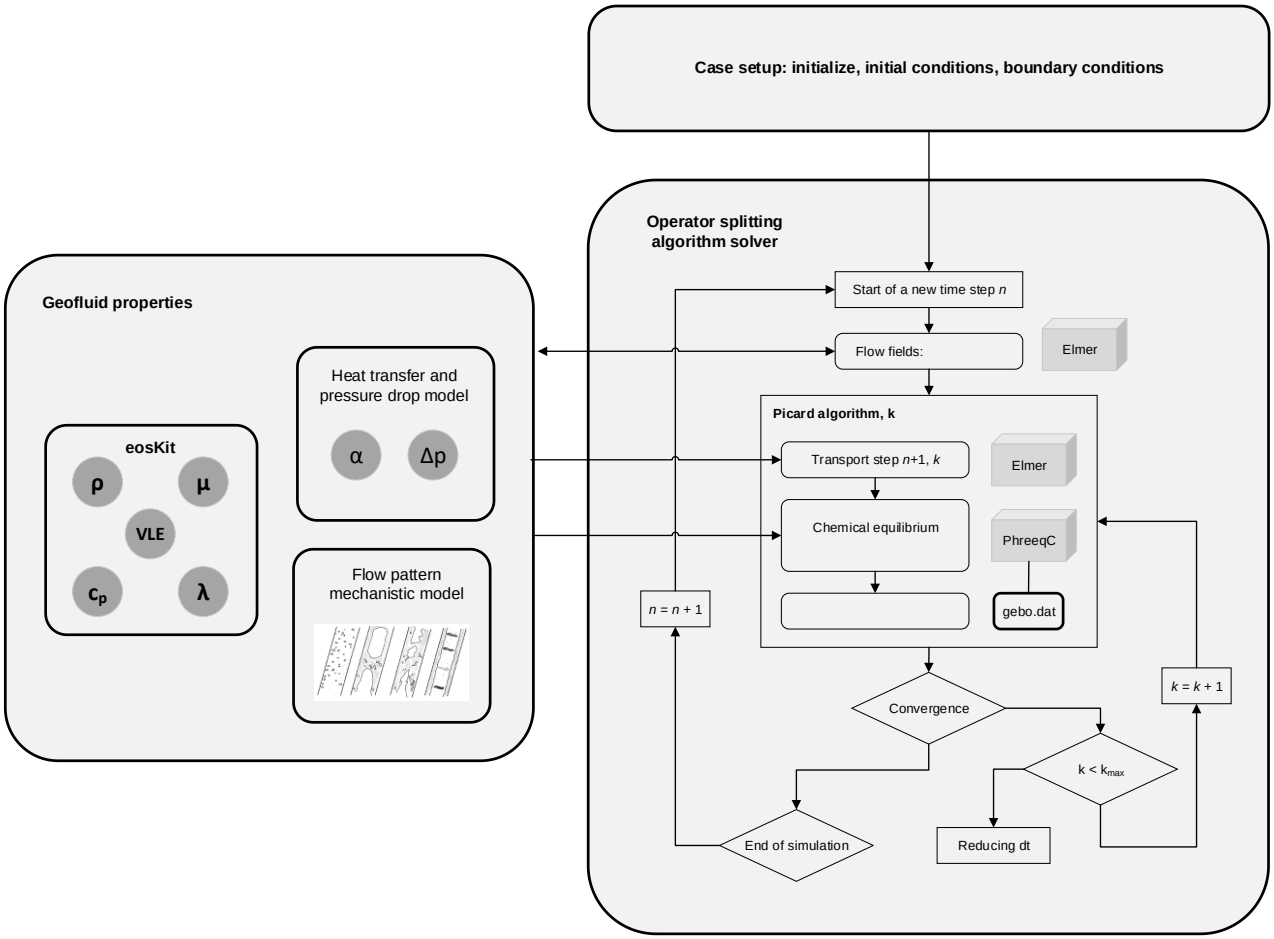

Figure 1: Main structure and workflow of the simulation

Once the boundary conditions have been set, each solver step for a specified time step, consists of the following major sub-steps:

1. For definite salt and gas concentrations at each cell, chemical equilibrium is solved in PHREEQC to obtain the saturation index of minerals according to eqs. (1) to (4), which is then used to determine mineral scaling and to calculate the dissolved salt concentration in the aqueous phase.
2. Thermodynamic properties, i.e., aqueous and non-aqueous enthalpy h^{AQ}, h^{NA}; density ρ^{AQ}, ρ^{NA}; viscosity μ^{AQ}, μ^{NA}; thermal conductivity $\lambda^{AQ}, \lambda^{NA}$; gas fugacity ϕ_j, and quality x, are determined using the equation of state described in section 2.4 as a function of the pressure p(z), enthalpy h(z), and the salt b_i (z) and gas molality b_j (z), and gas mole fraction y_j (z).
3. Void fraction is determined, based on the flow-pattern map, mechanistic flow model from (H-K, 2010), which is the used to calculate the effective two-phase thermodynamic properties with eqs (5) to (8).
4. Geofluid heat and mass transfer, pressure drop, and ions transport are solved in with constitutive relations, i.e. heat transfer coefficient α, wall shear $\left(\frac{dp}{dz}\right)_f$, and hydrostatic pressure gradient $\left(\frac{dp}{dz}\right)_h$.
5. From Elmer calculation we retrieve temperature, ion, and gas fugacity fields, which are sent to PHREEQC for the equilibrium at the next time step.

3.2 Model validation

3.2.1 Fluid-rock heat transfer

The heat transfer between geofluid and rock in the vicinity is validated by using analytical solution from Wu-Pruess (1990) as shown below.

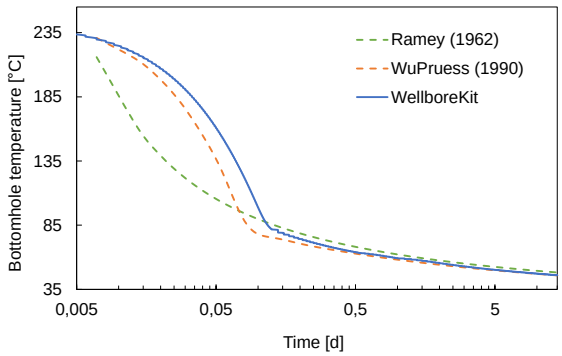

Figure 2: Heat transfer validation using analytical solutions.

3.2.2 Two-phase model

The two-phase flow model is validated by using code-to-code validation. Dymola (Dynamic Modeling Laboratory) was used to compare two-phase production of pure water, as depicted in Figure 3 below.

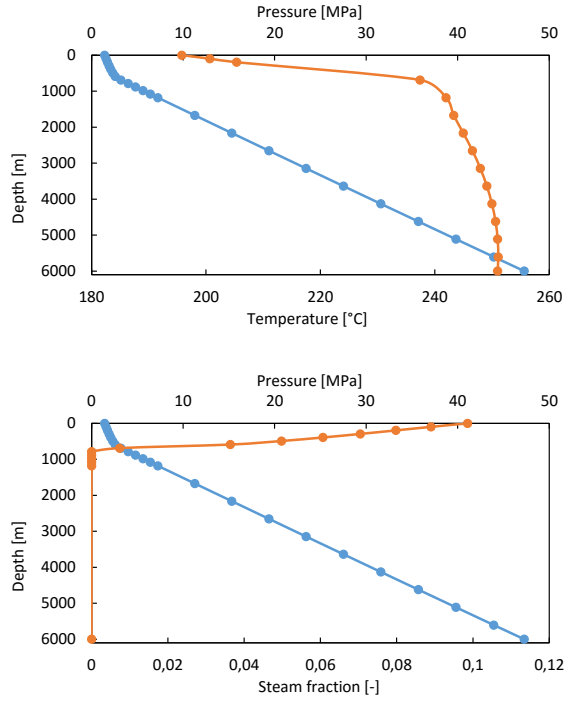

Figure 3: Comparison between numerical and analytical solution for cold injection case (a) Dymola results for the purpose of validation: Dynamic (a) Profiles at flow rate of 60 kg/s (c, d). Both used pure water properties.

3.2.3 Single-phase case study: Stimulations in Soulz-Sous-Forets

All figures and tables (beside the tables A-G at the end of the paper) should have a reference in the text, (Fig. x) or (Table x). They should be inserted as close as possible after the first reference to them, and should have a caption beneath them (in the case of figures) or above them (in the case of tables), as shown below.

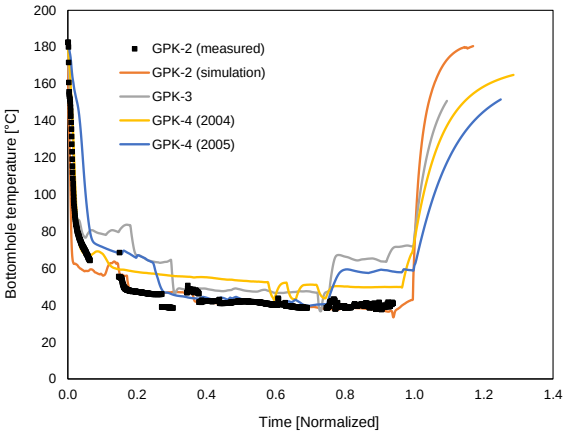

Figure 4: Heat transfer validation using analytical solutions.

4. GEOTHERMAL FLUID PRODUCTION AND INJECTION EXAMPLE

Sandia, working with ThermaSource Inc, a geothermal drilling contractor, developed tasks, time-, and cost descriptions of the construction process for a geothermal well (Polsky et al., 2008; Mansure et al., 2005). (Yost et al., 2015). The well is designed to generate 5 MWe from 80 kg/s of 200 °C wellhead fluid produced from a depth of 20,000 ft. [Note that we are using the foot, inches units since this was used in the Sandia Case.] In order to reach the designed depth of 20,000 ft, Sandia's well design (see Fig. 1) calls for five casing strings – a Surface Casing, an Intermediate Casing, and three production liners, labeled Production 1, Production 2, and Production 3. Each casing string overlaps the previous casing string by 200 ft. A tieback liner rests on top of the Intermediate Casing and fits within the Surface Casing in order to create a sealed, smooth conduit for injection of a working fluid.

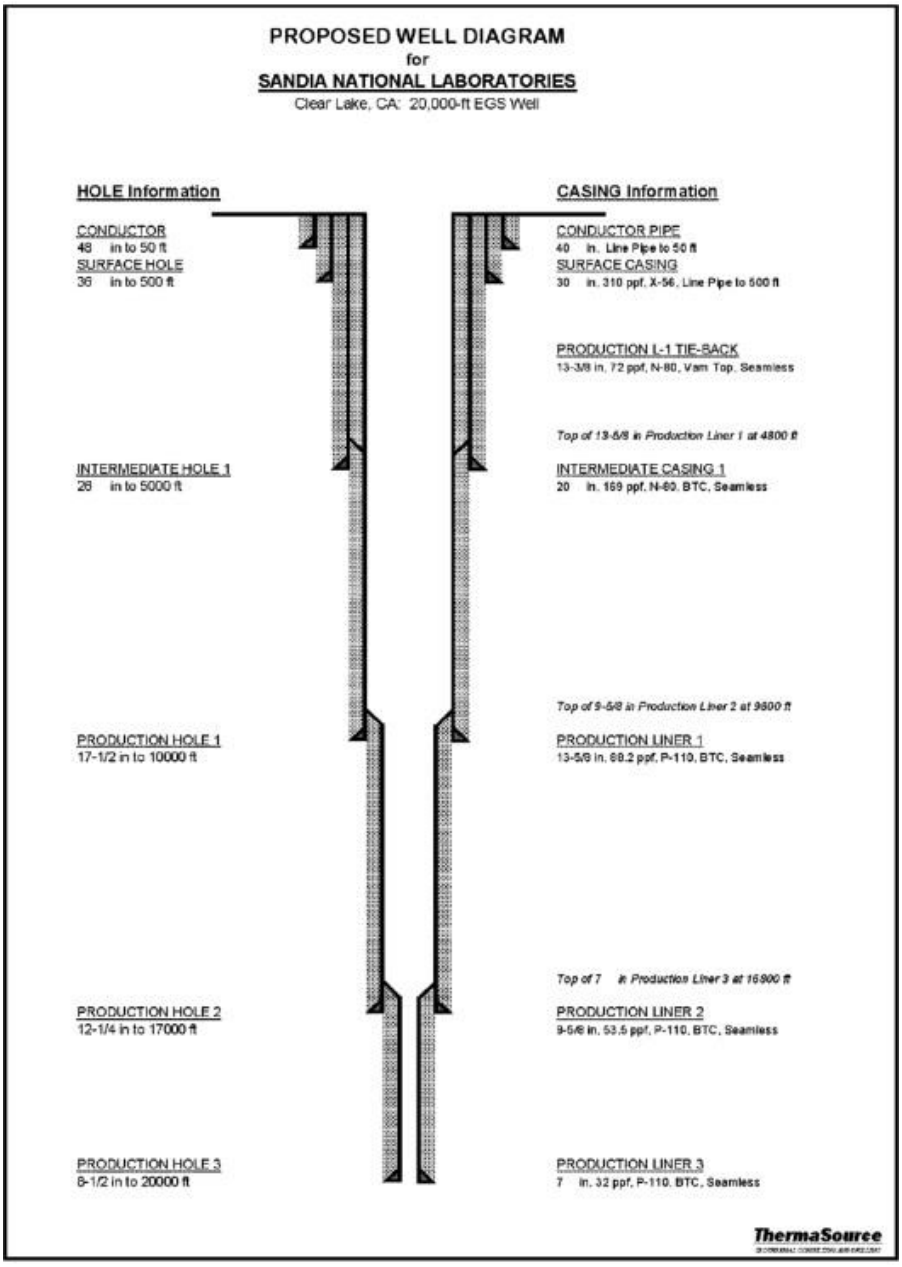

Figure 5: Unified Modeling Language (UML) diagram of the geothermal fluid model

A 1-D element can be used for the calculation of transport in tube-like structures that are surrounded by 2-D or 3-D matrix elements. Special intermediate elements ensure that no temperature variation is encountered in the pipe perpendicular to the flow direction. Furthermore, the impact of topography or hydraulic groundwater flow (forced or density-driven convection) on the thermal transport can be calculated in selected regions of the model domain (Kohl, 2002).

Since the annual temperature variations affect only the topmost 15 m, negligible with respect to the total wellbore depth range, a constant surface temperature of 15 ºC (annual mean) was taken as an upper boundary condition. The few borehole temperature measurements available prevent us from reaching a detailed definition of the subsurface and allowed only to perform homogeneous considerations.

The geometry of the wellbore system allows us to assume axial symmetry around the center of the system so that we can perform 3-D simulations by 2-D geometry (radius r, depth z). It is necessary to take into account the axial effects that are caused by the surface and bottom boundaries of the wellbore.

Heat transfer in the inclined borehole is also a three-dimensional problem. Therefore, the temperature responses on the inclined wellbore wall perimeter of any cross-section perpendicular to its axis are unequal and vary with the borehole depth. It can be concluded from Ping, 2006 that the variation of the temperature on the inclined borehole wall along its depth was almost similar to that on the vertical borehole. This illustrates that inclined borehole can be modeled as vertical borehole for simplicity of two-dimensional problem.

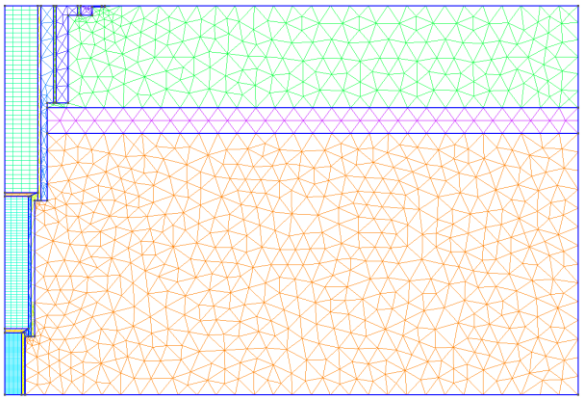

Figure 6: A quasi-2D wellbore model

The final FE mesh was discretized in 50 m steps (see coarse discretization in Fig. 1) in a vertical direction along the borehole, with a refinement in its lower part in order to reduce the numerical instabilities that can easily occur here. At a vertical and horizontal distance from the borehole, the mesh was quickly coarsened. In a horizontal direction next to the borehole, the tubing assembly was matched to a distance of 10 m. At larger lateral distances, a successively coarser mesh was generated.

The 1-D flow geometry in the tubing was simulated by lower dimensioned 1-D tube elements by setting the thermal conductivity in the vertical direction into arbitrary high value, which is capable of calculating accurately thermal advection at high fluid flow rates and accounting exactly for flow velocity changes at different diameters. Flow-pattern (mechanistic) with gas-exsolution effect.

4.1 Impact of slip correlation

An assumption of no slip between the phases is likely to be a somewhat coarse simplification. However, to establish which slip relation is better suited for geofluid wellbore depressurizations is outside the scope of the present work. Nevertheless, as an illustration of the effect that the slip relation may have, calculations have been performed employing the Hasan-Kabir relation.

4.2 Impact of geofluid composition

To show the influence of the mixture composition, several different mixtures have been considered.

4.3 Impact of wall friction

Roughness due to precipitation, corrosion, inner diameter reduction due to precipitation should be taken into account. In this section, we will test the effect of employing the friction model for the wall friction force in the momentum (2) and energy equation (3).

4.4 Impact of production or injection rate

In this section, we will examine the effect of different mass flow rate in the momentum (2) and energy equation (3) on the pressure, temperature, and mineral saturation indices.

5. CONCLUSIONS

The intent of this work was to establish a simulation platform by setting up a series of numerical models of a deep geothermal system to help design a power plant coupled with medium-temperature geothermal fluid resources. In this study, the wellbore models were developed by the thermohydraulic and chemical analysis. The wellbore model was validated by comparing its results with the reference data from published literature. Geometric configurations of the wellbores designed were determined by applying the operating conditions obtained from the system simulation to the design requirements. The performance of the wellbores was evaluated regarding the geofluid compositions, slip ratio between aqueous and non-aqueous phases and frictional pressure drop. It is anticipated that, based on the design tool platform, the modeling and design of an efficient, cost-effective wellbore can be carried out to exploit effectively deep geothermal fluid resources to generate electricity.

We have proposed to employ a two-phase, multi-component, heterogeneous drift-flux model for the transport and de-/pressurization of geofluid mixtures. Calculations have been performed for a mixture using the improved Duan-Sun model equation of state to compute the mixture properties. The operator splitting approach scheme was employed for the numerical solution of the thermohydro-chemical model and produced accurate results even for this complex model. It should be noted, however, that the accuracy of the model itself depends on constitutive relations like the slip relation, heat-transfer model and wall friction model, which need to be further studied for deep geothermal applications. The present results confirm that the mixture composition influences the pressure propagation speed and the amount of cooling exerted by depressurization. These issues should be taken into account for the design and operation of geothermal systems.

REFERENCES

Megel, T. (Ed.) (2005): Downhole Pressures Derived from Wellhead Measurements during Hydraulic Experiments. With assistance of T. Kohl, A. Gerard, L. Rybach, R. Hopkirk. World Geothermal Congress. Antalya, 24-29 April. GEOWATT AG. Turkey.

Ramey, H. J., Jr. (1962): Wellbore Heat Transmission. In Journal of Petroleum Technology 14 (4). DOI: 10.2118/96-PA.

Wu, Yu-Shu; Pruess, Karsten (2013): An Analytical Solution for Wellbore Heat Transmission in Layered Formations (includes associated papers 23410 and 23411). In SPE Reservoir Engineering 5 (04), pp. 531–538. DOI: 10.2118/17497-PA

Hasan, A.R., Kabir, C.S., 2002. Fluid flow and heat transfer in wellbores. Textbook Series, SPE, Richardson, Texas.